International Journal of Innovative
Computing, Information and Control
Volume **17**, Number **5**, October **2021**

ICIC International ©2021 ISSN 1349-4198
pp. 1705–1716

UNCONSTRAINED CONTINUOUS CONTROL SET MODEL PREDICTIVE CONTROL BASED ON KALMAN FILTER FOR ACTIVE POWER FILTER

Jianfeng Yang*, Yang Liu* and Zheng Li

School of Automation and Electrical Engineering
Lanzhou Jiaotong University
No. 88, Anning West Road, Anning District, Lanzhou 730070, P. R. China
*Corresponding authors: jfyang@lzjtu.edu.cn; 0619406@stu.lzjtu.edu.cn
0219402@stu.lzjtu.edu.cn

Received March 2021; revised July 2021

Abstract. *In the life and industrial power, due to the nonlinear load and new energy grid, many harmonics will be generated, which will reduce the power quality. Active power filter (APF) is the most used device in harmonic suppression, so it is very important to improve the rapidity and steady-state performance of APF. Model predictive control (MPC) appears with industry. It has been successfully applied in motor, power electronic converter and so on. Continuous control set model predictive control (CCS-MPC) is widely used in power industry because of its good control effect, CCS-MPC uses the predictive model, and the minimization cost function is calculated at each moment to obtain the output sequence in N time horizon in the future. In this paper, a CCS-MPC with dynamic feedback based on Kalman observer is proposed to overcome the influence of unmeasurable disturbance on the output of the system in industrial environment. Compared with the traditional model with disturbance term, it has the characteristics of small amount of calculation and fast response. The simulation results show that it has a good ability to deal with interference, and also has a good steady-state performance.*
Keywords: Active power filter, Continuous control set model predictive control, Kalman observer

1. **Introduction.** In the weak current network, a variety of new energy for grid connected power generation, and when many nonlinear power electronic devices and equipment are in operation, it will produce a lot of harmonics and pollute the power quality. The decline of power quality will cause power system failure and lead to power accidents, affect the safety of electricity. Since APF was proposed, it has been widely used in harmonic and reactive power compensation [1,2].

For the control of APF, including AC inner loop control and DC side voltage control, the DC side generally uses PI control. AC side is the key technology of APF control, which largely determines its compensation effect. Many control methods have been proposed for AC inner loop control. In [3], a hierarchical repetitive control method is proposed to improve the dynamic performance of APF. In [4], a neural network control method for APF is proposed, which improves the compensation accuracy of APF. The structure of APF without harmonic detection is proposed in [5], which improves the accuracy of APF. In [6], an adaptive robust predictive current control method is proposed. Model predictive control (MPC) is a method with the emergence and rapid development of the industry. It is quickly used in power electronic devices. [7] proposed a finite set model predictive control method, which has a fast dynamic response, but the switching frequency is not

DOI: 10.24507/ijicic.17.05.1705

fixed. In [8], the receiving horizon model predictive control for a three-phase voltage source inverter (VSI) is proposed. The cost function is established and the optimal duty cycle is generated by using space vector modulation. It can work at a fixed switching frequency and has a fast dynamic response. However, its embedded integrated Kalman filter further increases the amount of calculation.

In this paper, a model predictive control method based on discrete state-space model is proposed. The unmeasurable disturbance is extended to the state variable of the model, and its magnitude and influence on the output are estimated by the Kalman filter to control the AC measurement of APF. Aiming at the discrete state-space model of APF, the state prediction and output prediction are carried out, and the real-time feedback coefficient is solved to obtain the control increment. Unconstrained CCS-MPC does not need to establish the weight matrix and output matrix, which avoids the selection and optimization of its weight coefficient, and does not need to establish the constraints on the state quantity and output increment. In the process of calculating the feedback coefficient and solving the control increment in real time, it can quickly get the feedback coefficient and follow the detected three-phase harmonics in time, which ensures the real-time and dynamic performance of APF control. Through the establishment of simulation, the effectiveness and feasibility of the theoretical method are verified.

In this paper, the simulation model of the entire system is established and compared with the without Kalman filter to verify the superiority of the with Kalman filter in three-phase APF. The remaining structure of this paper includes the following parts, the second section introduces the three-phase two-level APF model and the harmonic current detection method, the third section introduces the unconstrained CCS-MPC, the fourth section introduces the Kalman filter for CCS-MPC, and the fifth section shows the performance and results of the two control methods through simulation results. The sixth part is the conclusion.

2. Structure and Mathematics of APF.

CCS-MPC uses the dynamic mathematical model of the plant to predict the output of p (prediction horizon) time in the future at the current time, and compares the predicted value with the reference value [9-11], by establishing the cost function and solving the cost function to obtain the input at each time, the future m (control horizon) input can be obtained. In the application of converter, PWM modulation is needed to fix the switching frequency, and the first group of the control sequence is applied to the converter, and such a process is carried out at each time cycle, so it is also called receding-horizon model predictive control [12-14].

Figure 1 shows the system main circuit structure of a parallel APF compensation voltage source type nonlinear load, where e_a, e_b, e_c are grid voltage, i_{ca}, i_{cb}, i_{cc} are the output compensation current of APF, i_{La}, i_{Lb}, i_{Lc} are load current, where L and R are the filter inductance and equivalent resistance, C is DC side capacitance, which stores energy for bidirectional flow of APF and grid energy, for U_{dc} of the DC voltage hold stability.

In the three-phase static coordinate system, assuming the three-phase symmetry, according to Kirchhoff's current law, the dynamic expression of Equation (1) can be obtained, where u_{ca}, u_{cb}, and u_{cc} are the output voltage of APF.

$$\begin{cases} L\frac{\mathrm{d}i_a}{\mathrm{d}t} = e_a - Ri_a - u_{ca} \\ L\frac{\mathrm{d}i_b}{\mathrm{d}t} = e_b - Ri_b - u_{cb} \\ L\frac{\mathrm{d}i_c}{\mathrm{d}t} = e_c - Ri_c - u_{cc} \end{cases} \tag{1}$$

According to the differential equations of voltage and current flow in APF, the time horizon differential equation is transformed into a state space model. The state and input

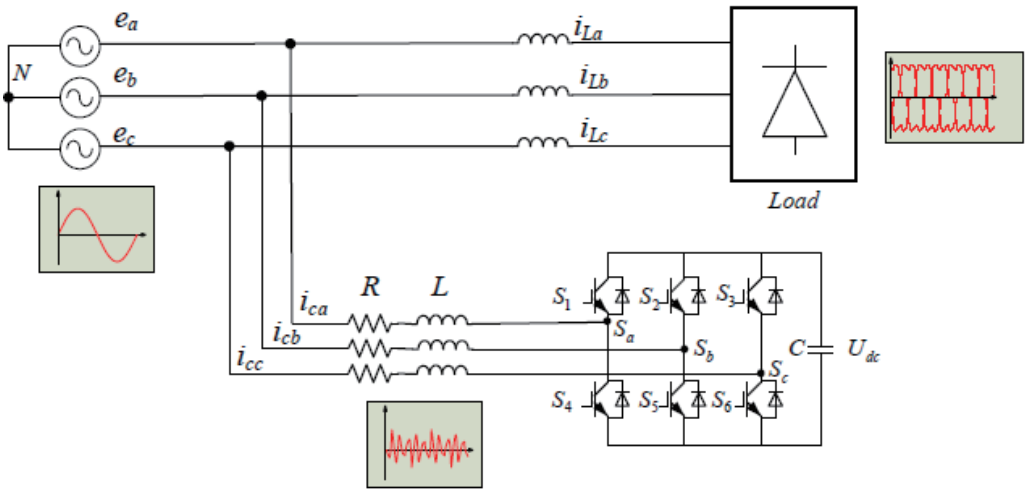

FIGURE 1. Three-phase APF topology diagram

are defined as $X = [i_a; i_b; i_c]$ and $U = [e_a - u_{ca}; e_b - u_{cb}; e_c - u_{cc}]$, so the new mathematical model is

$$\dot{\boldsymbol{X}} = A\boldsymbol{X} + B\boldsymbol{U} \tag{2}$$

where

$$A = \begin{bmatrix} -\frac{R}{L} & & \\ & -\frac{R}{L} & \\ & & -\frac{R}{L} \end{bmatrix}, \quad B = \begin{bmatrix} \frac{1}{L} & & \\ & \frac{1}{L} & \\ & & \frac{1}{L} \end{bmatrix}$$

By discretizing, the APF discretized state-space model of Equation (3) can be obtained.

$$\boldsymbol{X}(k+1) = \tilde{A}\boldsymbol{X}(k) + \tilde{B}\boldsymbol{U}(k) \tag{3}$$

where

$$\tilde{A} = e^{AT_s}, \quad \tilde{B} = \left(e^{AT_s} - I\right) A^{-1} B$$

Calculation of reference current. When APF is used to compensate harmonics and reactive power, it must be detected first, including FFT, FBD, PQ method, and so on. At present, the most widely used i_p-i_q detection method proposed by Akagi is that the fundamental wave of load current is obtained by filtering, and the harmonic content of load current can be obtained by subtracting the load current [2]. The DC side capacitor voltage of APF is controlled by PI, and the compensation part is injected to keep the energy interaction between AC measurement and DC side and stabilize it at the reference value. It has better dynamic performance and tracking performance, and the specific principle is shown in Figure 2 [18].

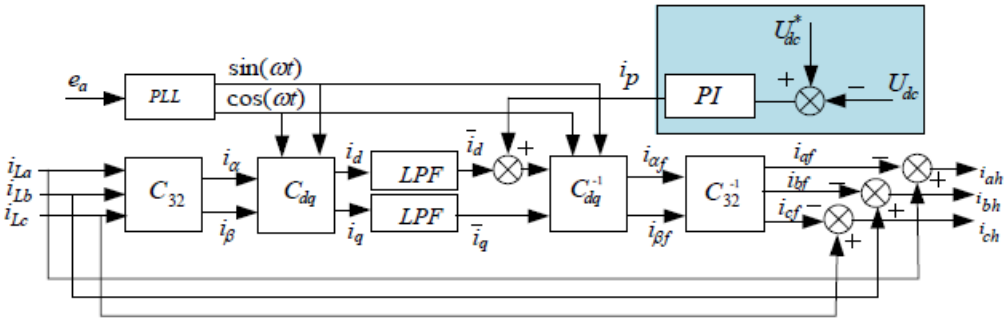

FIGURE 2. i_p-i_q method for harmonic detection of the reference current

According to the principle of APF, the detected harmonics need to be injected into the power grid in reverse, and then the APF outputs the harmonics of the same component. Therefore, it is necessary to take the harmonics as the reference value of APF and define $\boldsymbol{X}_{ref} = [i_{ah}; i_{bh}; i_{ch}]$. Harmonic detection uses phase locked loop (PLL) to detect phase and coordinate transformation, low-pass filter filtering, coordinate inverse transformation, which will inevitably produce delay, making the generated reference value lag about one cycle. In order to improve the accuracy of the reference value, it is necessary to predict the reference value at the next moment. In this paper, Lagrange interpolation prediction method is used, and the 2-order is taken.

$$\boldsymbol{X}_{ref}(k+1) = \sum_{i=0}^{n} (-1)^{n-i} \frac{(n+1)!}{i!(n+1-i)!} \cdot \boldsymbol{X}_{ref}(k+i-n) \tag{4}$$

3. Unconstrained CCS-MPC for APF.

3.1. Establishment of predictive model.

The diagram of APF's current predictive control is shown in Figure 3. i_o is the predicted active current component value of APF, and $i^*(k)$ is the harmonic reference current now. Generally, the difference between the DC side and the reference value is used. In this paper, the power control is performed on the DC side, the voltage regulator is controlled by the PI regulator, and the compensation is performed together with the harmonics [3-5]. After minimizing the objective function, the optimal control sequence can be obtained, and the first group of the control sequence is applied to the optimization, control the APF output compensation current to track the harmonics at the current moment, and predict the next time reference signal.

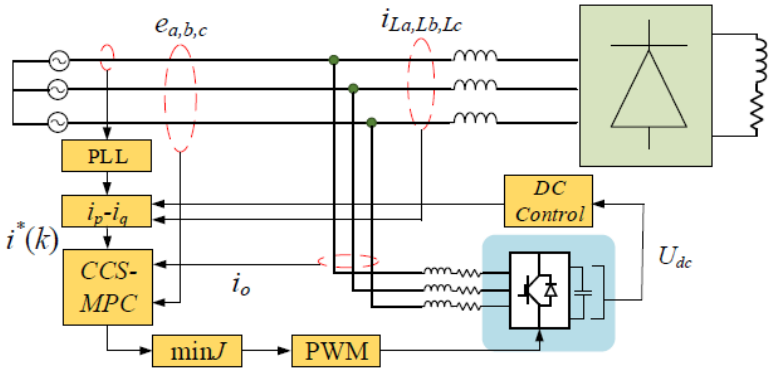

FIGURE 3. APF predictive control principle

According to Equation (2), in order to reduce the static error, the incremental model is adopted.

$$\begin{aligned} \boldsymbol{\Delta X}(k+1) &= \tilde{\boldsymbol{A}}\Delta\boldsymbol{X}(k) + \tilde{\boldsymbol{B}}\Delta\boldsymbol{U}(k) \\ \boldsymbol{Y}(k) &= \boldsymbol{C}\Delta\boldsymbol{X}(k) + \boldsymbol{Y}(k-1) \end{aligned} \tag{5}$$

where

$$\begin{aligned} \Delta\boldsymbol{X}(k) &= \boldsymbol{X}(k) - \boldsymbol{X}(k-1) \\ \Delta\boldsymbol{U}(k) &= \boldsymbol{U}(k) - \boldsymbol{U}(k-1) \end{aligned}$$

Let the prediction horizon be p and the control horizon be m. Through recursive iteration, we can get Equation (6). $k+1|t$ represents the prediction of the next time at

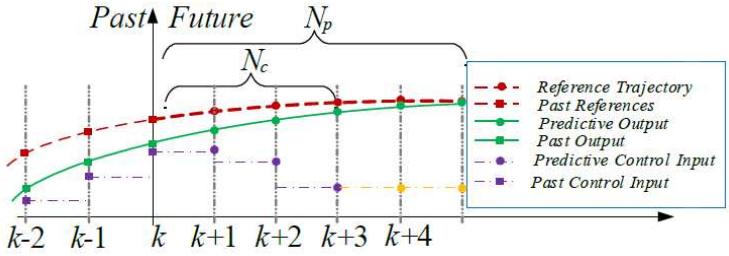

FIGURE 4. CCS-MPC method

time t, so we can predict the state from $k+m$ to $k+p$.

$$\begin{aligned}
\Delta \boldsymbol{X}(k+1|t) &= \tilde{\boldsymbol{A}}\Delta \boldsymbol{X}(k|t) + \tilde{\boldsymbol{B}}\Delta \boldsymbol{U}(k|t) \\
\Delta \boldsymbol{X}(k+2|t) &= \tilde{\boldsymbol{A}}\Delta \boldsymbol{X}(k+1|t) + \tilde{\boldsymbol{B}}\Delta \boldsymbol{U}(k+1) \\
&= \tilde{\boldsymbol{A}}^2\Delta \boldsymbol{X}(k|t) + \tilde{\boldsymbol{A}}\tilde{\boldsymbol{B}}\Delta \boldsymbol{U}(k|t) + \tilde{\boldsymbol{B}}\Delta \boldsymbol{U}(k+1|t) \\
&\vdots \\
\Delta \boldsymbol{X}(k+p|t) &= \tilde{\boldsymbol{A}}\Delta \boldsymbol{X}(k+p-1|t) + \tilde{\boldsymbol{B}}\Delta \boldsymbol{U}(k+p-1|t) \\
&= \tilde{\boldsymbol{A}}^p\Delta \boldsymbol{X}(k|t) + \tilde{\boldsymbol{A}}^{p-1}\tilde{\boldsymbol{B}}\Delta \boldsymbol{U}(k|t) + \tilde{\boldsymbol{A}}^{p-2}\tilde{\boldsymbol{B}}\Delta \boldsymbol{U}(k+1|t) + \cdots \\
&\quad + \tilde{\boldsymbol{A}}^{p-m-1}\tilde{\boldsymbol{B}}\Delta \boldsymbol{U}(k+m-1|t)
\end{aligned} \tag{6}$$

Similarly, the $\boldsymbol{Y}(k+p|t)$ can be obtained:

$$\begin{aligned}
\boldsymbol{Y}(k+p|t) = &\sum_{i=1}^{p} \tilde{\boldsymbol{C}}\tilde{\boldsymbol{A}}^i\Delta \boldsymbol{X}(k|t) + \sum_{i=1}^{p} \tilde{\boldsymbol{C}}\tilde{\boldsymbol{A}}^{i-1}\tilde{\boldsymbol{B}}\Delta \boldsymbol{U}(k|t) + \cdots \\
&+ \sum_{i=1}^{p-m+1} \tilde{\boldsymbol{C}}\tilde{\boldsymbol{A}}^{i-1}\tilde{\boldsymbol{B}}\Delta \boldsymbol{U}(k+m-1|t) + \boldsymbol{Y}(k|t)
\end{aligned} \tag{7}$$

According to Equations (6) and (7), the prediction model can be written as:

$$\boldsymbol{Y}(k+1) = \boldsymbol{\Psi}_t\Delta \boldsymbol{X}(k) + \boldsymbol{\Theta}_t\Delta \boldsymbol{U}(k) + \boldsymbol{I}\boldsymbol{Y} \tag{8}$$

where

$$\boldsymbol{Y}(k+1) = \begin{bmatrix} \boldsymbol{Y}(k+1|t) \\ \vdots \\ \boldsymbol{Y}(k+p|t) \end{bmatrix},\ \boldsymbol{\Psi}_t = \begin{bmatrix} \tilde{\boldsymbol{C}}\tilde{\boldsymbol{A}} \\ \vdots \\ \sum_{i=1}^{p} \tilde{\boldsymbol{C}}\tilde{\boldsymbol{A}}^i \end{bmatrix},\ \Delta \boldsymbol{U}(k) = \begin{bmatrix} \Delta \boldsymbol{U}(1|t) \\ \vdots \\ \Delta \boldsymbol{U}(k+m-1|t) \end{bmatrix},$$

$$\boldsymbol{I} = \begin{bmatrix} I_{n_c\times n_c} \\ I_{n_c\times n_c} \end{bmatrix},\ \boldsymbol{\Theta}_t = \begin{bmatrix} \tilde{\boldsymbol{C}}\tilde{\boldsymbol{B}} & 0 & 0 & 0 \\ \vdots & \vdots & \ddots & \vdots \\ \sum_{i=1}^{m} \tilde{\boldsymbol{C}}\tilde{\boldsymbol{A}}^{i-1}\tilde{\boldsymbol{B}} & \sum_{i=1}^{m-1} \tilde{\boldsymbol{C}}\tilde{\boldsymbol{A}}^{i-1}\tilde{\boldsymbol{B}} & \cdots & \tilde{\boldsymbol{C}}\tilde{\boldsymbol{A}}\tilde{\boldsymbol{B}} \\ \vdots & \vdots & \ddots & \vdots \\ \sum_{i=1}^{p} \tilde{\boldsymbol{C}}\tilde{\boldsymbol{A}}^{i-1}\tilde{\boldsymbol{B}} & \sum_{i=1}^{p-1} \tilde{\boldsymbol{C}}\tilde{\boldsymbol{A}}^{i-1}\tilde{\boldsymbol{B}} & \cdots & \tilde{\boldsymbol{C}}\tilde{\boldsymbol{A}}^{p-1}\tilde{\boldsymbol{B}} \end{bmatrix}$$

3.2. **Establishment of objective function.** CCS-MPC with dynamic feedback does not add a constraint matrix, but adds a weight matrix to the state and input, which does not affect the off-line calculation. First, the weight factor of each state quantity is set as $\boldsymbol{Q} = \mathrm{diag}[\boldsymbol{q}_1, \boldsymbol{q}_2, \ldots, \boldsymbol{q}_p]$, $\boldsymbol{q}_i = \mathrm{diag}[q_1, q_2, \ldots, q_{nc}]$. The reference is $\boldsymbol{R}(k+1) = [\boldsymbol{X}_{ref}(k+1), \boldsymbol{X}_{ref}(k+2), \ldots, \boldsymbol{X}_{ref}(k+p)]$.

The cost function of Equation (9) is adopted in order to avoid too large control action. $\boldsymbol{H} = \mathrm{diag}[h_1, h_2, \ldots, h_m]$, $\boldsymbol{h}_i = \mathrm{diag}[h_1, h_2, \ldots, h_{nc}]$ is the weight factors of the input increment.

$$J = \sum_{i=1}^{p} \|\boldsymbol{q}_i(\boldsymbol{X}_{ref}(k+1) - \boldsymbol{Y}(k+1))\|^2 + \sum_{i=1}^{m} \|\boldsymbol{h}_i \Delta \boldsymbol{U}(k+i-1)\|^2 \tag{9}$$

$\boldsymbol{h}_i$ is the weight factor of all control increments of the i-th prediction. According to the cost function (9), we can get an optimization problem (10).

$$\min_{\Delta U(k)} J(\boldsymbol{X}(k), \Delta \boldsymbol{U}(k), m, p) \tag{10}$$

3.3. **Optimization problem solving.** In order to make the predicted value track the harmonic reference value, the error of the next time can be obtained, and the open-loop optimization problem can be solved, the optimal control sequence at k time can be obtained as Equation (11).

$$\min_{\Delta U(k)} J(\boldsymbol{X}(k), \Delta \boldsymbol{U}(k), m, p) = \|\boldsymbol{q}_i(\boldsymbol{X}_{ref}(k+1) - \boldsymbol{Y}(k+1))\|^2 + \|\boldsymbol{h}_i \Delta \boldsymbol{U}(k+i-1)\|^2 \tag{11}$$

We can define auxiliary variables:

$$\rho \stackrel{\text{def}}{=} \begin{bmatrix} \boldsymbol{q}_i(\boldsymbol{X}_{ref}(k+1) - \boldsymbol{Y}(k+1)) \\ \boldsymbol{h}_i \Delta \boldsymbol{U}(k+i-1) \end{bmatrix} \tag{12}$$

So the optimization problem can be expressed as:

$$\min_{\Delta U(k)} J(\boldsymbol{X}(k), \Delta \boldsymbol{U}(k), m, p) = \rho^{\mathrm{T}} \rho \tag{13}$$

Solve it and we can obtain:

$$\boldsymbol{E}_p(k+1) = \boldsymbol{X}_{ref}(k+1) - \boldsymbol{\Psi}_t \Delta \boldsymbol{X}(k) - \boldsymbol{I}\boldsymbol{Y}(k) \tag{14}$$

$$\Delta \boldsymbol{U}^*(k) = \left(\boldsymbol{\Theta}^{\mathrm{T}} \boldsymbol{Q}^{\mathrm{T}} \boldsymbol{Q} \boldsymbol{\Theta} + \boldsymbol{H}^{\mathrm{T}} \boldsymbol{H}\right)^{-1} \boldsymbol{\Theta}^{\mathrm{T}} \boldsymbol{Q}^{\mathrm{T}} \boldsymbol{Q} \boldsymbol{E}_p(k+1) \tag{15}$$

According to the principle of MPC, only the first control sequence is selected, the control gain $\boldsymbol{g}_{mpc}$ can be defined as:

$$\boldsymbol{g}_{mpc} = [\ \mathbf{I}_{nc \times nc} \quad 0 \quad \ldots \quad 0\ ] \times \left(\boldsymbol{\Theta}^{\mathrm{T}} \boldsymbol{Q}^{\mathrm{T}} \boldsymbol{Q} \boldsymbol{\Theta} + \boldsymbol{H}^{\mathrm{T}} \boldsymbol{H}\right)^{-1} \boldsymbol{\Theta}^{\mathrm{T}} \boldsymbol{Q}^{\mathrm{T}} \boldsymbol{Q} \boldsymbol{E}_p(k+1) \tag{16}$$

In the next moment, the process is continuously carried out, and the first group of input increment at each moment is

$$\Delta \boldsymbol{u}(k) = \boldsymbol{g}_{mpc} \boldsymbol{E}_p(k+1) \tag{17}$$

4. **Kalman Filter for CCS-MPC.** The state variable $x(k)$ of the Kalman filter for discrete-time process estimation is a recursive estimation algorithm. Suppose that the state-space model is Equation (18), u is the input variable, w is the process noise, v is the observation noise, and A, B, and H are all gain matrices.

$$\begin{aligned} x_k &= Ax_{k-1} + Bu_{k-1} + w_{k-1} \\ z_k &= Hx_k + v_k \end{aligned} \tag{18}$$

Both w and v are Gaussian white noise, which accords with a normal distribution.

$$\begin{aligned} p(w) &\sim N(0, Q) \\ p(v) &\sim N(0, R) \end{aligned} \tag{19}$$

Kalman filter uses the feedback method to estimate process state, which is divided into two parts: time update, and measurement update. Time update is mainly used for prediction, which is responsible for estimating the current state variables and error covariance and providing a priori estimation for the next time. The measurement update is used as a correction to provide a posteriori estimation for the next time. The time renewal equation is

$$\begin{aligned} \hat{x}_k^- &= A\hat{x}_{k-1}^- + Bu_{k-1} \\ P_k^- &= AP_{k-1}^- A^T + Q \end{aligned} \tag{20}$$

The measurement renewal equation is

$$\begin{aligned} K_k &= P_k^- H^T \left(HP_k^- H^T + R\right)^{-1} \\ \hat{x}_k &= \hat{x}_k^- + K_k \left(z_k - H\hat{x}_k^-\right) \\ P_k &= (I - K_k H)P_k^- \end{aligned} \tag{21}$$

At the next time, the time update equation and the measurement update equation are solved repeatedly, and the posterior estimation obtained from the last calculation is taken as the prior estimation of the next calculation. The process is shown in Figure 5.

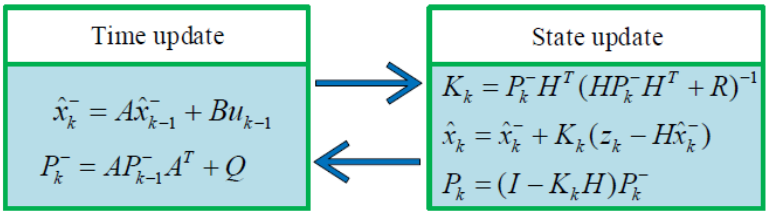

FIGURE 5. Kalman filter principal diagram

4.1. **Kalman filter with CCS-MPC.** Because in the actual system, the harmonic detection process needs to detect the grid voltage, load current, etc., the unknown disturbance will interfere with the measurement results and affect the reference value. After adding the disturbance term in the MPC, we can get a new mathematical model as follows.

$$\begin{aligned} \boldsymbol{\Delta X}(k+1) &= \tilde{\boldsymbol{A}}\Delta \boldsymbol{X}(k) + \tilde{\boldsymbol{B}}\Delta \boldsymbol{U}(k) + \tilde{\boldsymbol{B}}_d \Delta \boldsymbol{d}(k) \\ \boldsymbol{Y}(k) &= \boldsymbol{C}\Delta \boldsymbol{X}(k) + \boldsymbol{Y}(k-1) \end{aligned} \tag{22}$$

$$\boldsymbol{d}(k) = C_d \boldsymbol{X}_{ref}(k) \tag{23}$$

So

$$\begin{aligned} \Delta \boldsymbol{X}(k+p|t) &= \tilde{\boldsymbol{A}}\Delta \boldsymbol{X}(k+p-1|t) + \tilde{\boldsymbol{B}}\Delta \boldsymbol{U}(k+p-1|t) + \tilde{\boldsymbol{B}}_d \Delta \boldsymbol{d}(k+p-1|t) \\ &= \tilde{\boldsymbol{A}}^p \Delta \boldsymbol{X}(k|t) + \tilde{\boldsymbol{A}}^{p-1}\tilde{\boldsymbol{B}}\Delta \boldsymbol{U}(k|t) + \tilde{\boldsymbol{A}}^{p-2}\tilde{\boldsymbol{B}}\Delta \boldsymbol{U}(k+1|t) + \cdots \\ &\quad + \tilde{\boldsymbol{A}}^{p-m-1}\tilde{\boldsymbol{B}}\Delta \boldsymbol{U}(k+m|t) + \tilde{\boldsymbol{A}}^{p-1}\tilde{\boldsymbol{B}}_d \Delta \boldsymbol{d}(k) \end{aligned} \tag{24}$$

And the predictive output in $k+p$ is

$$\begin{aligned} \boldsymbol{Y}(k+p|t) = &\sum_{i=1}^{p} \tilde{\boldsymbol{C}}\tilde{\boldsymbol{A}}^i \Delta \boldsymbol{X}(k|t) + \sum_{i=1}^{p} \tilde{\boldsymbol{C}}\tilde{\boldsymbol{A}}^{i-1}\tilde{\boldsymbol{B}}\Delta \boldsymbol{U}(k|t) + \cdots \\ &+ \sum_{i=1}^{p-M+1} \tilde{\boldsymbol{C}}\tilde{\boldsymbol{A}}^{i-1}\tilde{\boldsymbol{B}}\Delta \boldsymbol{U}(k+m-1|t) \end{aligned} \tag{25}$$

$$+\sum_{i=1}^{p}\tilde{\boldsymbol{C}}\tilde{\boldsymbol{A}}^{i-1}\tilde{\boldsymbol{B}}_d\Delta\boldsymbol{d}(k|t)+\boldsymbol{Y}(k|t)$$

And $\boldsymbol{E}_p(k+1)$ is

$$\boldsymbol{E}_p(k+1)=\boldsymbol{X}_{ref}(k+1)-\boldsymbol{\Psi}_t\Delta\boldsymbol{X}(k)-\boldsymbol{I}\boldsymbol{Y}(k)-\boldsymbol{\Psi}_d\Delta\boldsymbol{d}(k) \tag{26}$$

where

$$\boldsymbol{\Psi}_d=\begin{bmatrix}\tilde{\boldsymbol{C}}\tilde{\boldsymbol{B}}_d\\ \vdots\\ \sum_{i=1}^{p}\tilde{\boldsymbol{C}}\tilde{\boldsymbol{A}}^{i-1}\tilde{\boldsymbol{B}}_d\end{bmatrix}$$

The control principle is as the following Figure 6.

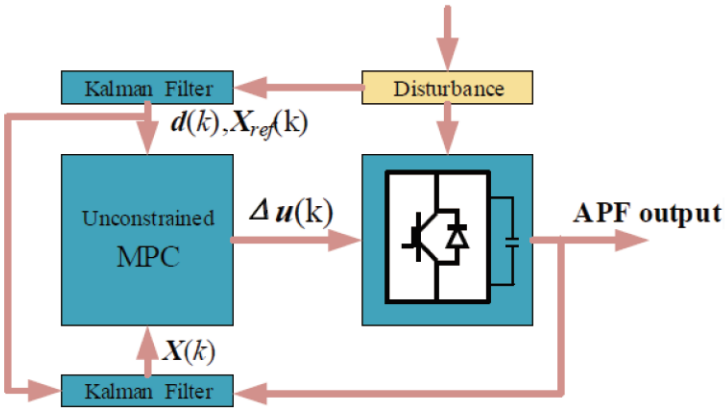

FIGURE 6. Kalman filter with CCS-MPC

In the presence of interference, in order to get the ideal state value, it is necessary to detect the relevant variables effectively. As shown in Figure 6, using a Kalman filter to detect the load current can get the ideal harmonic reference current and interference estimation value. At the same time, using the Kalman filter to observe the output of APF, the estimated value of the state can be obtained and fed back to MPC controller. Finally, the output value is applied to APF to complete the control of APF under unmeasurable interference.

5. **Simulation and Results Analysis.** In order to verify the ability of CCS-MPC with dynamic feedback based on Kalman filter to deal with noise and unknown disturbance, built it in MATLAB/Simulink, parameters are shown in Table 1. The load changes in 0.3 seconds, and the reference current is the harmonics detected by i_p-i_q method. And in the presence of interference, compare with the control mode without Kalman filter.

In order to obtain a good control effect, reduce the amount of computation, set $p=20$ and the $m=6$. In this section, the advantages of CCS-MPC with dynamic feedback based on Kalman filter in the presence of interference are compared when the parameter settings are the same.

Figure 7(a) shows the load current before compensation, which is seriously distorted due to the existence of nonlinear load, low order harmonics (5, 7, 11, 13) are dominant, total harmonic distortion (THD) is 20.58%, and it cannot meet the requirements of the power grid, less than 5%. Figure 7(b) shows performance of CCS-MPC with dynamic feedback without Kalman filter, which does not deal with disturbances. In Figure 7(c), it shows the performance of dealing with disturbance, (c) is closer to the sine wave, and it

TABLE 1. Simulation model parameters

Parameters	Value
Grid voltage	380 V
DC voltage	800 V
Capacitor C	3000 μF
Inductor	4 mH
Resistor	0.01 Ω
Load resistor	10 Ω

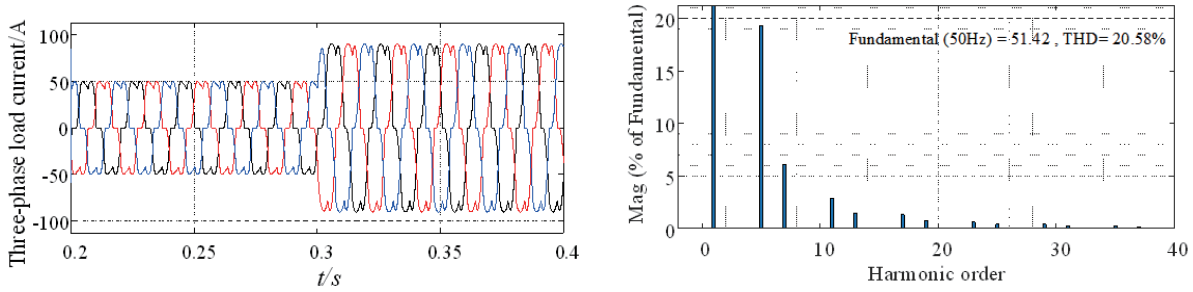

(a) Load current and THD

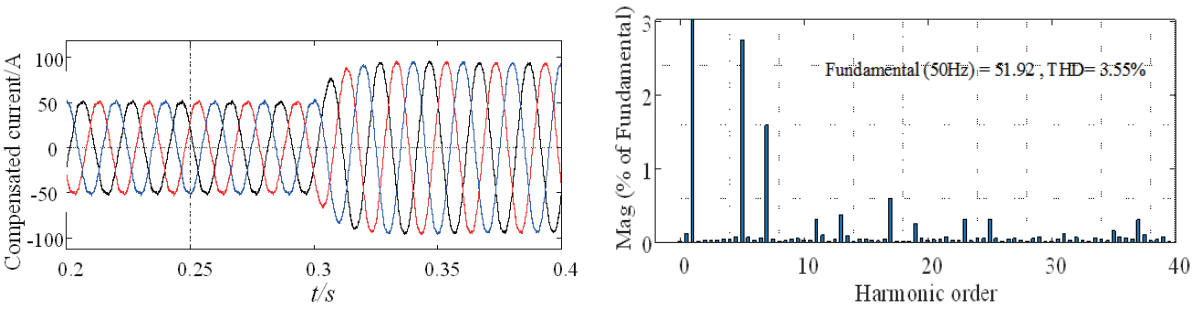

(b) Unconstrained CCS-MPC without Kalman filter

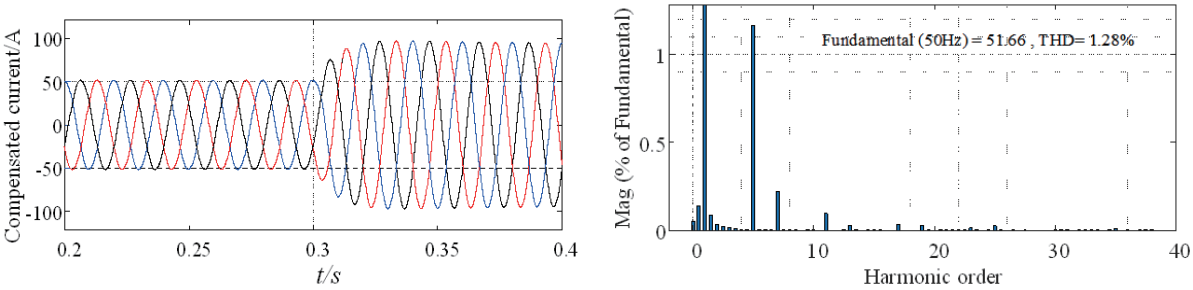

(c) Unconstrained CCS-MPC with Kalman filter

FIGURE 7. Three-phase current and THD under two methods

has the lower THD. Obviously, after processing the measurement disturbance, combined with a good control method, APF can have better compensation performance.

Figures 8(a) and 8(b) describe what the APF tracks the harmonic reference value in two ways, the method of (b) has better tracking effect, and can better compensate the harmonic of power grid. As shown above, when controlling the operation of APF, with the Kalman filter get a better performance; in other words, in the industrial environment, the unknown disturbance will have less impact on the performance of APF.

$\boldsymbol{E}_p(k+1)$ represents the error between the future reference value and the predicted value, when set to 0.25, start APF, as we can see in Figure 9, when it is not started, its

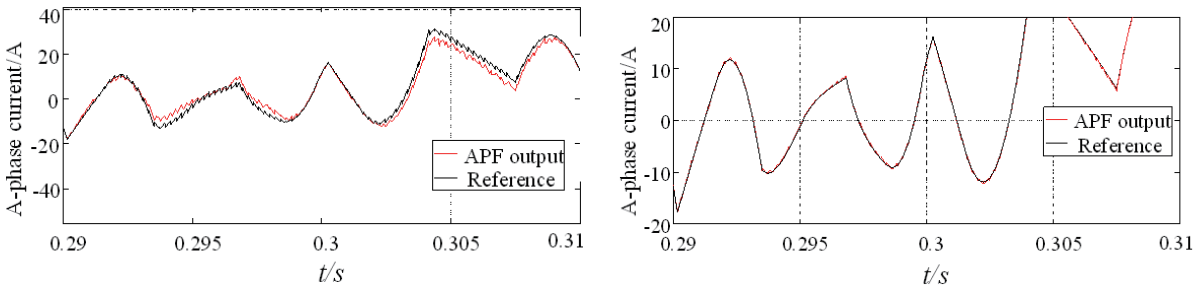

(a) Tracking without Kalman filter (b) Tracking with Kalman filter

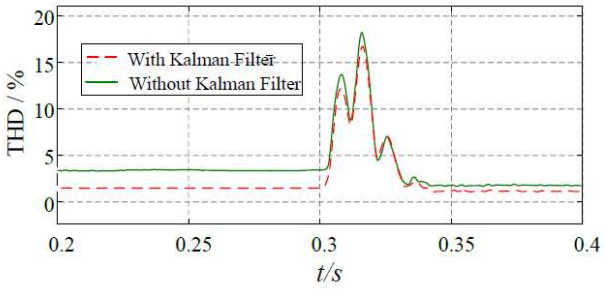

(c) Comparison of THD changes

FIGURE 8. Three-phase current tracking and THD changes under two methods

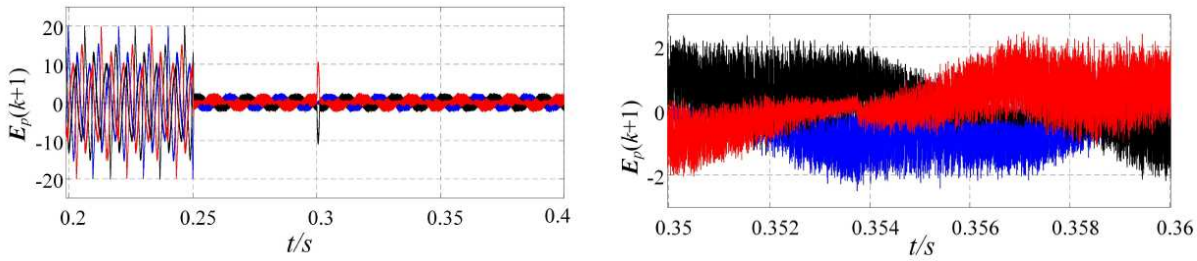

(a) $\boldsymbol{E}_p(k+1)$ on unconstrained CCS-MPC without Kalman filter

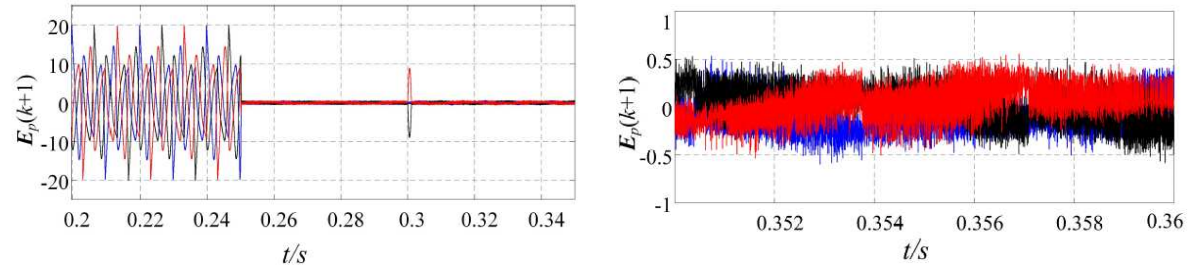

(b) $\boldsymbol{E}_p(k+1)$ on unconstrained CCS-MPC with Kalman filter

FIGURE 9. Three-phase current errors under two methods

value is relatively large. After the start of APF, the predictive error of a method is larger because of the disturbance, after using the Kalman filter to observe the measured value and state value, as shown in Figure 9(b), the error $\boldsymbol{E}_p(k+1)$ is reduced from the original amplitude of 2 to 0.5.

From the results in Figure 9, it can be found that the proposed method in this paper, which combines the fast dynamic response of unconstrained CCS-MPC with less computation and the disturbance processing of the Kalman filter, significantly improves the

performance of APF, especially in the unknown industrial environment, because in the complex field environment, the measurement device will be unreliable.

6. **Conclusion.** In this paper, an unconstrained CCS-MPC based on the Kalman filter is proposed, compared with the traditional CCS-MPC, the unconstrained CCS-MPC has the characteristics of real-time feedback and less computation, which is equivalent to off-line control, lower requirements on the processor, and further reduces the delay. However, in the industrial environment and field application, the unreliability of the measurement device will interfere with the harmonic detection and the state of the controller and reduce the performance of APF. In this paper, the Kalman filter is used to solve the unknown disturbance and improve the performance of APF. As the main equipment to compensate harmonics and reactive power, this control method can be further applied in APF in the future.

Acknowledgment. This work is supported by the National Natural Science Foundation of China (Grant number: 61863023).

REFERENCES

[1] B. Singh, K. Al-Haddad and A. Chandra, A review of active filters for power quality improvement, *IEEE Transactions on Industrial Electronics*, vol.46, no.5, pp.960-971, doi: 10.1109/41.793345, 1999.

[2] H. Akagi, New trends in active filters for power conditioning, *IEEE Transactions on Industry Applications*, vol.32, no.6, pp.1312-1322, doi: 10.1109/28.556633, 1996.

[3] A. Garcia-Cerrada, O. Pinzon-Ardila, V. Feliu-Batlle, P. Roncero-Sanchez and P. Garcia-Gonzalez, Application of a repetitive controller for a three-phase active power filter, *IEEE Transactions on Power Electronics*, vol.22, no.1, pp.237-246, doi: 10.1109/TPEL.2006.886609, 2007.

[4] D. O. Abdeslam, P. Wira, J. Merckle, D. Flieller and Y. Chapuis, A unified artificial neural network architecture for active power filters, *IEEE Transactions on Industrial Electronics*, vol.54, no.1, pp.61-76, doi: 10.1109/TIE.2006.888758, 2007.

[5] Q. Trinh and H. Lee, An advanced current control strategy for three-phase shunt active power filters, *IEEE Transactions on Industrial Electronics*, vol.60, no.12, pp.5400-5410, doi: 10.1109/TIE.2012.2229677, 2013.

[6] J. M. Espi, J. Castello, R. García-Gil, G. Garcera and E. Figueres, An adaptive robust predictive current control for three-phase grid-connected inverters, *IEEE Transactions on Industrial Electronics*, vol.58, no.8, pp.3537-3546, doi: 10.1109/TIE.2010.2089945, 2011.

[7] J. G. L. Foster, R. R. Pereira, R. B. Gonzatti, W. C. Sant'Ana, D. Mollica and G. Lambert-Torres, A review of FCS-MPC in multilevel converters applied to active power filters, *2019 IEEE 15th Brazilian Power Electronics Conference and the 5th IEEE Southern Power Electronics Conference (COBEP/SPEC)*, Santos, Brazil, pp.1-6, doi: 10.1109/COBEP/SPEC44138.2019.9065398, 2019.

[8] R. Guzman, L. G. de Vicuña, A. Camacho, J. Miret and J. M. Rey, Receding-horizon model-predictive control for a three-phase VSI with an LCL filter, *IEEE Transactions on Industrial Electronics*, vol.66, no.9, pp.6671-6680, doi: 10.1109/TIE.2018.2877094, 2019.

[9] S. Kouro, P. Cortes, R. Vargas, U. Ammann and J. Rodriguez, Model predictive control – A simple and powerful method to control power converters, *IEEE Transactions on Industrial Electronics*, vol.56, no.6, pp.1826-1838, doi: 10.1109/TIE.2008.2008349, 2009.

[10] J. Rodriguez et al., State of the art of finite control set model predictive control in power electronics, *IEEE Transactions on Industrial Informatics*, vol.9, no.2, pp.1003-1016, doi: 10.1109/TII.2012.2221469, 2013.

[11] J. Rodriguez et al., Predictive current control of a voltage source inverter, *IEEE Transactions on Industrial Electronics*, vol.54, no.1, pp.495-503, doi: 10.1109/TIE.2006.888802, 2007.

[12] S. Kwak and J. Park, Switching strategy based on model predictive control of VSI to obtain high efficiency and balanced loss distribution, *IEEE Transactions on Power Electronics*, vol.29, no.9, pp.4551-4567, doi: 10.1109/TPEL.2013.2286407, 2014.

[13] R. P. Aguilera, P. Lezana and D. E. Quevedo, Switched model predictive control for improved transient and steady-state performance, *IEEE Transactions on Industrial Informatics*, vol.11, no.4, pp.968-977, doi: 10.1109/TII.2015.2449992, 2015.

[14] H. Akagi, Y. Kanazawa and A. Nabae, Instantaneous reactive power compensators comprising switching devices without energy storage components, *IEEE Transactions on Industry Applications*, vol.IA-20, no.3, pp.625-630, doi: 10.1109/TIA.1984.4504460, 1984.

[15] S. R. Mohapatra and V. Agarwal, A low computational cost model predictive controller for grid connected three phase four wire multilevel inverter, *2018 IEEE 27th International Symposium on Industrial Electronics (ISIE)*, Cairns, QLD, pp.305-310, doi: 10.1109/ISIE.2018.8433727, 2018.

[16] T. Jin, X. Shen, T. Su and R. C. C. Flesch, Model predictive voltage control based on finite control set with computation time delay compensation for PV systems, *IEEE Transactions on Energy Conversion*, vol.34, no.1, pp.330-338, doi: 10.1109/TEC.2018.2876619, 2019.

[17] C. Bordons and C. Montero, Basic principles of MPC for power converters: Bridging the gap between theory and practice, *IEEE Industrial Electronics Magazine*, vol.9, no.3, pp.31-43, doi: 10.1109/MIE.2014.2356600, 2015.

[18] Y. Zhang, J. Hu and J. Zhu, Three-vectors-based predictive direct power control of the doubly fed induction generator for wind energy applications, *IEEE Transactions on Power Electronics*, vol.29, no.7, pp.3485-3500, doi: 10.1109/TPEL.2013.2282405, 2014.

[19] W. Budiharto, Intelligent controller of electric wheelchair from manual wheelchair for disabled person using 3-axis joystick, *ICIC Express Letters, Part B: Applications*, vol.12, no.2, pp.201-206, doi: 10.24507/icicelb.12.02.201, 2021.